



# 1 Early Pliocene vegetation and hydrology changes in western 2 equatorial South America

3 Friederike Grimmer<sup>1</sup>, Lydie Dupont<sup>1</sup>, Frank Lamy<sup>2</sup>, Gerlinde Jung<sup>1</sup>, Catalina González<sup>3</sup>, Gerold Wefer<sup>1</sup>

4 <sup>1</sup>MARUM – Center for Marine Environmental Sciences, University of Bremen, Leobener Str. 8, 28359 Bremen, Germany

5 <sup>2</sup>Alfred-Wegener-Institute for Polar and Marine Research, Am Handelshafen 12, 27570 Bremerhaven, Germany

6 <sup>3</sup>Department of Biological Sciences, Universidad de los Andes, Cra. 1 #18a-12, Bogotá, Colombia

7 *Correspondence to:* Friederike Grimmer (fgrimmer@marum.de)

8 **Abstract.** During the early Pliocene, two major tectonic events triggered a profound reorganization of ocean and atmospheric  
9 circulation in the Eastern Equatorial Pacific (EEP), the Caribbean Sea, and on adjacent land masses: the progressive closure  
10 of the Central American Seaway (CAS) and the uplift of the northern Andes. These affected amongst others the mean  
11 latitudinal position of the Intertropical Convergence Zone (ITCZ). The direction of an ITCZ shift however is still debated, as  
12 numeric modelling results and paleoceanographic data indicate shifts in opposite directions. To provide new insights into this  
13 debate, an independent hydrological record of western equatorial South America was generated. Vegetation and climate of this  
14 area were reconstructed by pollen analysis of 46 samples from marine sediment core ODP 1239A from the EEP comprising  
15 the interval between 4.7 and 4.2 Ma. The study site is sensitive to latitudinal ITCZ shifts insofar as a southward (northward)  
16 shift would result in increased (decreased) precipitation over Ecuador. The presented pollen record comprises representatives  
17 from five ecological groups: lowland rainforest, lower montane forest, upper montane forest, páramo, and broad range taxa. A  
18 broad tropical rainforest coverage persisted in the study area throughout the early Pliocene, without significant open vegetation  
19 below the forest line. Between 4.7 and 4.42 Ma, humidity increases, reaching its peak around 4.42 Ma, and slightly decreasing  
20 again afterwards. The stable, permanently humid conditions are rather in agreement with paleoceanographic data indicating a  
21 southward shift of the ITCZ, possibly in response to CAS closure. The presence of páramo vegetation indicates that the Western  
22 Cordillera of the northern Andes had already reached considerable elevation by the early Pliocene. Future studies could extend  
23 the hydrological record of the region further back into the late Miocene to see if a more profound atmospheric response to  
24 tectonic changes occurred earlier.

## 25 1 Introduction

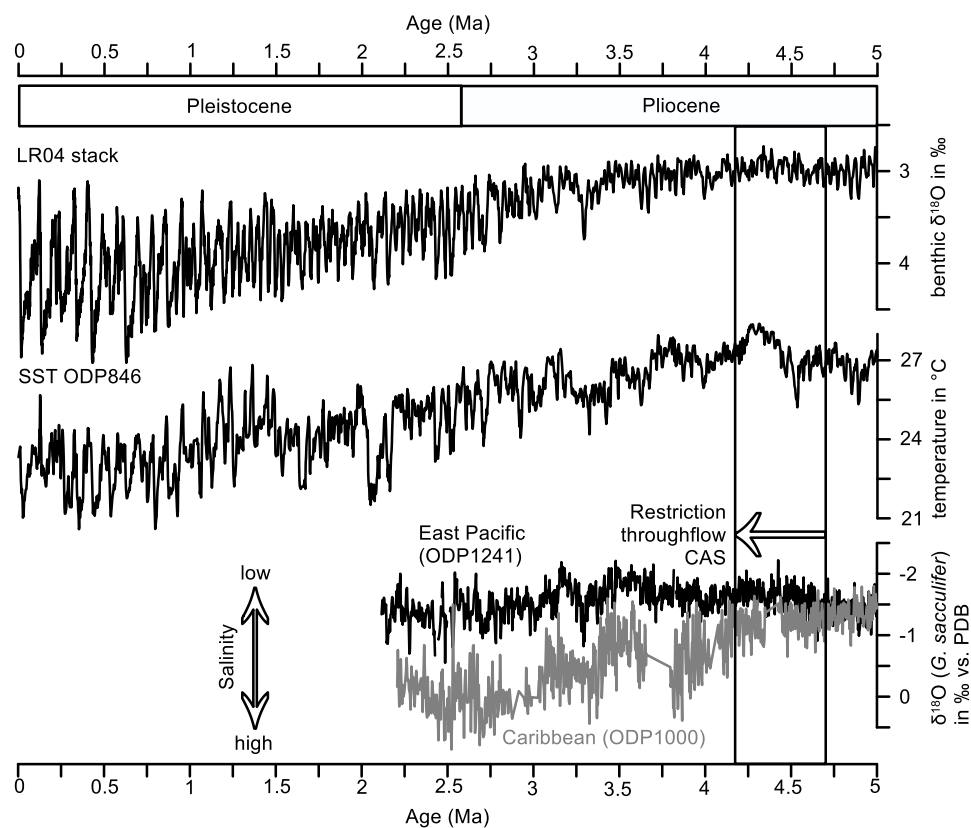
26 The Pliocene epoch is characterized by some profound tectonic processes which altered oceanic and atmospheric circulation  
27 on a regional and possibly also global scale (Cannariato and Ravelo, 1997; Lunt et al., 2008). Two of these processes are the  
28 closure of the Isthmus of Panama and the uplift of the northern Andes. The formation of the Isthmus of Panama, and especially  
29 the precise temporal constraints of the closure of the Panama Strait, have been subject of numerous studies (Bartoli et al., 2005;  
30 Groeneveld et al., 2014; Hoorn and Flantua, 2015; Montes, 2015; Steph, 2005). A recent review based on geological,



31 paleontological, and molecular records narrowed the formation *sensu stricto* down to 2.8 Ma (O’Dea et al., 2016). Temporal  
32 constraints on the restriction of the surface water flow through the gateway were established by salinity reconstructions on  
33 both sides of the Isthmus (Steph et al., 2006b, Fig. 1). The salinities first start to diverge around 4.5 Ma. A major step in the  
34 seaway closure between 4.7 and 4.2 Ma was also assumed based on the comparison of mass accumulation rates of the carbonate  
35 sand-fraction in the Caribbean Sea and the EEP (Haug and Tiedemann, 1998). The closure of the Central American Seaway  
36 has been associated with the development of the EEP cold tongue (EEP CT), strengthened upwelling in the EEP, the shoaling  
37 of the thermocline, and a mean latitudinal shift of the ITCZ (Steph, 2005; Steph et al., 2006a; Steph et al., 2006b; Steph et al.,  
38 2010). The direction of a potential shift of the ITCZ is still debated because of a discrepancy between paleoclimate  
39 reconstructions based on proxy data and numerical modelling results.

40 For the late Miocene, a northernmost paleoposition of the ITCZ at about 10–12°N has been proposed (Flohn, 1981; Hovan,  
41 1995). Subsequently, a southward shift towards 5°N paleolatitude between 5 and 4 Ma is indicated by eolian grain-size  
42 distributions in the eastern tropical Pacific (Hovan, 1995). Billups et al. (1999) provide additional evidence for a southward  
43 shift of the ITCZ between 4.4 and 4.3 Ma. Hence, most proxy data agree about a southward ITCZ shift during the early  
44 Pliocene. On the contrary, results from numerical modelling suggest a northward shift of the ITCZ in response to CAS closure  
45 (Steph et al., 2006b) and Andean uplift (Feng and Poulsen, 2014; Takahashi and Battisti, 2007).

46 An independent record of the terrestrial hydrology for the early Pliocene from a study site that is sensitive to latitudinal ITCZ  
47 shifts could provide new insights to this debate. Schneider et al. (2014) also stress the need of reconstructions of the ITCZ in  
48 the early and mid-Pliocene in order to understand how competing effects like an ice-free northern hemisphere and a weak EEP  
49 CT balanced, and to reduce uncertainties of predictions. Even though changes of ocean–atmosphere linkages related to ENSO  
50 (El Niño Southern Oscillation) and ITCZ shifts strongly impact continental precipitation in western equatorial South America,  
51 most studies so far have focused on paleoceanographic features such as sea surface temperatures and ocean stratification.



52

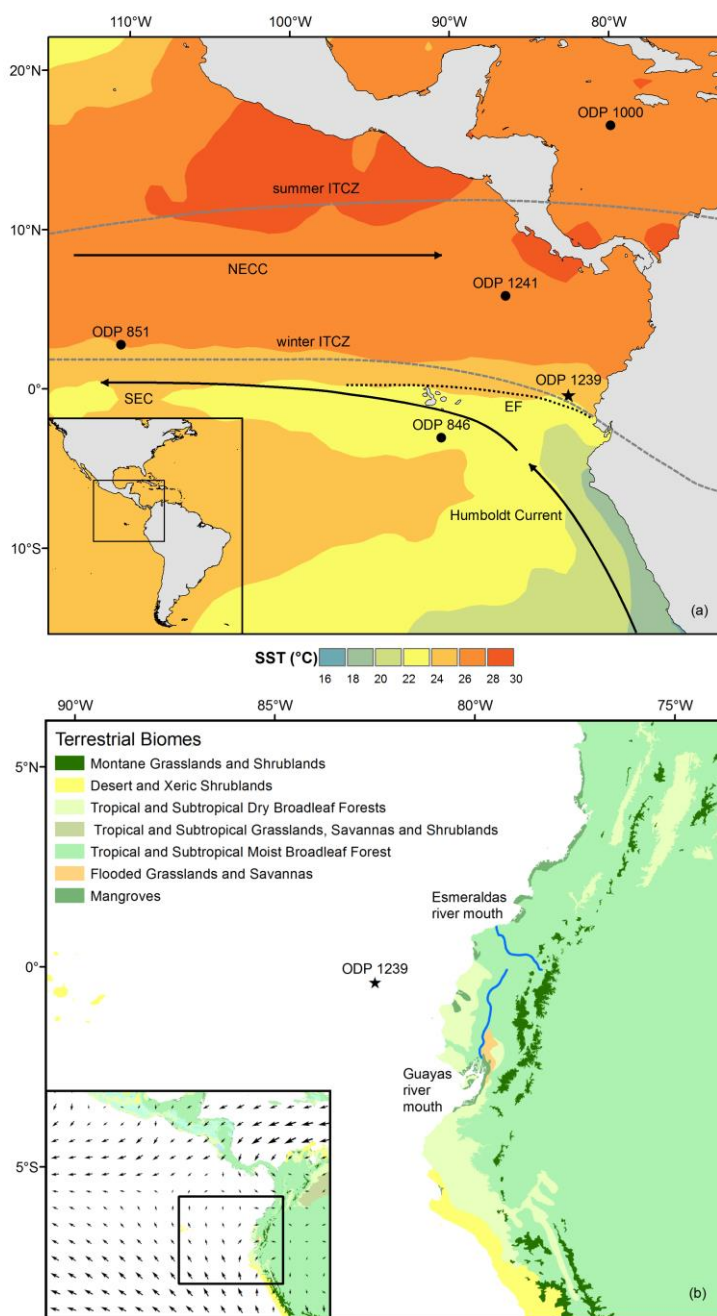
53 **Figure 1: LR04 global stack of benthic  $\delta^{18}\text{O}$  reflecting changes in global ice volume and temperature. Uk'37 sea surface temperatures**  
54 **(SST) of ODP Site 846 in the Equatorial Pacific Cold Tongue (Lawrence et al., 2006).  $\delta^{18}\text{O}$  of the planktonic foraminifer**  
55 ***G. sacculifer* from ODP Site 1000 in the Caribbean and ODP Site 1241 in the East Pacific (Steph, 2005; Steph et al., 2006a), reflecting changes in**  
56 **sea surface salinity (see Fig. 2 for location of ODP Sites). The box represents the time window analyzed in this study.**

57 The second major tectonic process is the uplift of the Northern Andes which strongly altered atmospheric circulation patterns  
58 over South America. Three major deformation phases include fan building in the lower Eocene to early Oligocene, compression  
59 of Oligocene deposits in the Miocene and Pliocene, and refolding during Pliocene to recent times (Corredor, 2003). While the  
60 uplift of the Central Andes is well investigated, only few studies deal with the timing of uplift of the Northern Andes. Coltorti  
61 and Ollier (2000), based on geomorphologic data, conclude that the uplift of the Ecuadorian Andes started in the early Pliocene  
62 and continued until the Pleistocene. More recent apatite fission track data indicate that the western Andean Cordillera of  
63 Ecuador was rapidly exhumed during the late Miocene (13–9 Ma) (Spikings et al., 2005). Uplift estimates for the Central  
64 Andes suggest that the Altiplano had reached less than half of its modern elevation by 10 Ma, with uplift rates increasing from  
65 0.1 mm/yr in the early and middle Miocene to 0.2–0.3 mm/yr to present. For the Eastern Cordillera of Colombia, elevations  
66 of less than 40% of the modern values are estimated for the early Pliocene, then increasing rapidly at rates of 0.5–3 mm/yr  
67 until modern elevations were reached around 2.7 Ma (Gregory-Wodzicki, 2000). Both the tectonic events and the closure of  
68 the Central American Seaway are assumed to have had a large impact on ocean and atmospheric circulation in the eastern



69 Pacific, the Caribbean and on adjacent land masses. Therefore, the reconstruction of continental climate, especially hydrology,  
70 will contribute to our understanding of climatic changes in this highly complex area.

71 To better understand the early Pliocene vegetation and hydrology of western equatorial South America we studied pollen and  
72 spores from the early Pliocene section (4.7–4.2 Ma) of the marine sediment record at ODP Site 1239 and compared this record  
73 to Holocene samples from the same Site. While other palynological studies of the region have been conducted for the mid-  
74 Pliocene to Holocene (González et al., 2006; Hooghiemstra, 1984; Seilles et al., 2016), this is the first palynological record of  
75 western equatorial South America from the early Pliocene. The record contributes to elucidate how vegetation and climate in  
76 this area responded to changes in atmospheric and oceanic circulation, possibly induced by the closure of the Central American  
77 Seaway and the uplift of the northern Andes. Therefore the main objectives of the study are firstly, to investigate long-term  
78 vegetation and climatic changes, focusing on hydrology, in western equatorial South America and, secondly, to interpret these  
79 changes in relation to climate phenomena influencing the hydrology of the region, especially the mean latitudinal position of  
80 the ITCZ and variability related to ENSO. These objectives are approached by the following research questions: 1) What floral  
81 and vegetation changes took place in the coastal plain and the Western Andean Cordillera of western equatorial South America  
82 from 4.7 to 4.2 Ma? 2) What are the climatic implications of the vegetation change, especially in terms of hydrology? 3) What  
83 are the implications for Andean uplift, especially regarding the development of the high Andean páramo vegetation?



84

85 **Figure 2: (a) Major oceanographic features of the eastern equatorial Pacific (SST: Sea surface temperature, statistical annual mean**  
 86 **from 2005-2012 from NOAA; NECC: North Equatorial Counter Current, SEC: South Equatorial Current, EF: Equatorial Front),**  
 87 **and boreal summer and winter position of the Intertropical Convergence Zone (ITCZ). The locations of ODP Sites mentioned in the**  
 88 **text are indicated. (b) Modern vegetation of western equatorial South America as defined by the World Wildlife Fund (please note**  
 89 **that the terrestrial biomes are not identical to the altitudinal vegetation belts shown in Fig. 3 and 4), major rivers draining into the**  
 90 **Pacific, and magnitude and direction of January surface winds (NCEP Reanalysis Derived monthly long term means from 1981-**  
 91 **2010 provided by the NOAA/OAR/ESRL PSD, Boulder, Colorado, USA, from their website at <http://www.esrl.noaa.gov/psd/>).**



## 92 **1.1 Modern setting**

### 93 **1.1.1 Climate and ocean circulation**

94 The climate of western equatorial South America is complex and heterogeneous, as it is not only controlled by large-scale  
95 tropical climate phenomena such as the ITCZ and the El Niño Southern Oscillation (ENSO), but is also strongly influenced by  
96 small-scale climate patterns caused by the diverse Andean topography. The annual cycle of precipitation in northwestern South  
97 America is controlled by insolation changes. During boreal summer when insolation is strongest in the northern hemisphere,  
98 the ITCZ is located at its northernmost position around 9°–10° N (Vuille et al., 2000). Approaching austral summer, the ITCZ  
99 moves southward across the equator. Within the range of the ITCZ, annual precipitation patterns are generally characterized  
100 by two minima and two maxima. The coastal areas of southern Ecuador where the ITCZ has its southernmost excursion show  
101 an annual precipitation pattern with one maximum during austral summer and a pronounced dry season during austral winter  
102 (Bendix and Lauer, 1992).

103 This general circulation pattern is modified by ENSO at interannual time-scales. During warm El Niño events, the lowlands  
104 of Ecuador experience abundant precipitation whereas the northwestern Ecuadorian Andes experience drought (Vuille et al.,  
105 2000). Regional climate patterns are also modified by the topography of the Andes which pose an effective barrier for the  
106 large-scale atmospheric circulation. While precipitation patterns east of the Andes are driven by moisture-laden easterly trade  
107 winds originating over the tropical Atlantic and the Amazon basin, the coastal areas and the western Andean slopes are  
108 dominated by air masses originating in the Pacific (Vuille et al., 2000, Fig. 2). The warm annual El Niño current which flows  
109 southward along the Colombian Pacific coast warms the air masses along the coast. This moist air brings over 6000 mm yearly  
110 precipitation to the northern coastal plain (Balslev, 1988). In contrast, the coastal areas of southernmost Ecuador and northern  
111 Peru are under the influence of the cold Humboldt Current which transports cold and nutrient rich waters and gives rise to a  
112 long strip of coastal desert. The westwards flow of the cold surface waters of the EEP CT to the western Pacific via the South  
113 Equatorial Current (SEC) is driven by the Walker Circulation. Warm waters return eastwards via the North Equatorial  
114 Countercurrent (NECC, see Fig. 2). An abrupt transition between the cold SEC and the warm NECC is the Equatorial Front  
115 (EF).

### 116 **1.1.2 Geography, vegetation and pollen transport**

117 The study area is geographically divided into three main regions: the coastal plain with several rivers draining into the Pacific,  
118 the Andes, and the eastern lowlands which constitute the western margin of the Amazon Basin. The mountains form two  
119 parallel cordilleras which are separated by the Interandean Valley. The diverse vegetation is the result of the combined effects  
120 of elevation and precipitation. In the coastal plain there is an abrupt shift from tropical lowland rainforests in the north to a  
121 desert dominated by annual xerophytic herbs in the south. This shift reflects the dependence of the vegetation on precipitation  
122 which ranges from 100 to 6000 mm per year on the coastal plain. The western slopes of the Andes are covered by montane  
123 forest, which is partly interrupted by drier valleys in southern Ecuador (Balslev, 1988).



124 Along the coast, mangrove stands occur in the salt- and brackish-water tidal zone of river estuaries and bays. They are formed  
125 by two species of *Rhizophora* (*R. harrisonii* and *R. mangle*), and to a lesser extent *Avicennia*, *Laguncularia*, and *Conocarpus*  
126 are present (Twilley et al., 2001). The lowland rainforest is characterized by the dominant plant families Fabaceae, Rubiaceae,  
127 Palmae, Annonaceae, Melastomataceae, Sapotaceae, and Clusiaceae in terms of species richness. In the understory, Rubiaceae,  
128 Araceae, and Piperaceae form the predominant elements (Gentry, 1986). In the lower montane forest, *Cyathea*, Meliaceae (e.g.  
129 *Ruagea*), Fabaceae (e.g. *Dussia*), Melastomataceae (e.g. *Meriania*, *Phainantha*), Rubiaceae (e.g. *Cinchona*), Proteaceae (e.g.  
130 *Roupala*), Lauraceae (e.g. *Nectandra*), and Pteridaceae (e.g. *Pterozonium*) are common elements. Upper montane forests are  
131 dominated by *Myrsine*, *Ilex*, *Weinmannia*, *Clusia*, *Schefflera*, *Myrcianthes*, *Hedyosmum*, and *Oreopanax* (Jørgensen et al.,  
132 1999).

133 Above ca. 3200 m, trees become sparse and eventually the vegetation turns into páramo. The páramo is a unique ecosystem of  
134 the high altitudes of the northern Andes of South America and of southern Central America, located between the continuous  
135 forest line and the permanent snowline at about 3000–5000 m (Luteyn, 1999). The grass páramo is formed by tussock grasses,  
136 mainly *Calamagrostis* and *Festuca*. These are complemented by shrubs of *Diplostephium*, *Hypericum*, and *Pentacalia*, and  
137 forest patches of *Polylepis*. The shrub páramo consists of cushion plants like *Azorella*, *Plantago*, and *Werneria*, and shrubs  
138 like *Loricaria* and *Chuquiraga*. The vegetation of the desert páramo is scarce. Some common taxa are *Nototriche*, *Draba*, and  
139 *Culcitium* (Sklenar and Jorgensen, 1999). The high rates of orographic precipitation that characterize the western part of  
140 equatorial South America cause pollen grains to be washed down by the rain quickly. Therefore, the main transport agent are  
141 the rivers draining into the Pacific. The northern coastal plain of Ecuador is mainly drained by the Esmeraldas and Santiago  
142 Rivers, and the southern coastal plain is drained by several smaller rivers which end in the Guayas River. From the river  
143 mouths, pollen might cross the Peru-Chile Trench in nepheloid layers to reach the Carnegie Ridge.

### 144 1.1.3 Drilling site

145 ODP Site 1239 is located at 0°40.32'S, 82°4.86'W, about 120 km offshore Ecuador in a water depth of 1414m, near the eastern  
146 crest of Carnegie Ridge and just next to a downward slope into the Peru-Chile Trench (Mix et al., 2003). Its location is close  
147 to the Equatorial Front (Fig. 2) which separates the warm and low-salinity waters of Panama Basin from the cooler and high-  
148 salinity surface waters of the EEP CT. The region of Site 1239 reveals a thick sediment cover, with dominant sediments in the  
149 region being foraminifer-bearing diatom nannofossil ooze. A tectonic backtrack path on the Nazca plate (Pisias, 1995) reveals  
150 a paleoposition of Site 1239 about 150–200 km further westward (away from the continent) and slightly southward relative to  
151 South America at 4–5 Ma compared to the present day position (Mix et al., 2003). The sediments of Carnegie Ridge are  
152 characterized by high smectite values. Due to its proximity to the Ecuadorian coast, Site 1239 is suitable to record changes in  
153 fluvial runoff, related to variations of precipitation in northwestern South America. Most of the material is discharged by the  
154 Guayas River and Esmeraldas River (Rincon-Martinez et al., 2010).



## 155 2 Methods

156 46 sediment samples of 10 cm<sup>3</sup> volume were taken at 67 cm intervals on average from ODP Hole 1239A (cores 33X5-37X1).  
157 Additionally, two core top samples were taken from ODP Hole 1239B as modern analogues. Standard analytical methods were  
158 used to process the samples, including decalcification with HCl (~10%) and removal of silicates with HF (~40%). Two tablets  
159 of exotic *Lycopodium* spores (batch #177,745 containing 18584 ± 829 spores per tablet) were added to the samples during the  
160 decalcification step for calculation of pollen concentrations (grains/cm<sup>3</sup>). After neutralization with KOH (40%) and washing,  
161 the samples were sieved with ultrasound over an 8µm screen to remove smaller particles. Samples were mounted in glycerin  
162 and a minimum of 100 pollen/spore grains (178 on average) were counted in each sample using a Zeiss Axioskop and 400x  
163 and 1000x (oil immersion) magnification.

164 For pollen identification, the Neotropical Pollen Database (Bush and Weng, 2007), a reference collection for Neotropical  
165 species held at the Department of Palynology and Climate Dynamics in Göttingen, and related literature (Colinvaux et al.,  
166 1999; Hooghiemstra, 1984; Murillo and Bless, 1974, 1978; Roubik and Moreno, 1991) were used. Pollen types were grouped  
167 according to their main ecological affinity (Flantua et al., 2014; Marchant et al., 2002). The zonation of the diagrams was  
168 based on constrained cluster analysis by sum-of-squares (CONISS), using the square root transformation method (Edwards &  
169 Cavalli-Sforza's chord distance) implemented in TILIA (Grimm, 1991) and visual inspection of the pollen percentage curves.  
170 Percentages are based on the pollen sum which includes all pollen and fern spore types including unidentifiables. Confidence  
171 intervals were calculated after Maher (1972). An initial age model for Site 1239 was established based on biostratigraphic  
172 information (Mix et al., 2003). The age model was refined by matching the benthic stable isotope records from Site 1239 with  
173 those from Site 1241 by visual identification of isotope stages. This procedure resulted in an indirectly orbitally tuned age  
174 age model for Site 1239, spanning the interval from 5 to 2.7 Ma (Tiedemann et al., 2007). A hiatus of ca. 5 meters exists between  
175 cores 35X and 36X of Hole 1239A (Tiedemann et al., 2007; Table AT3).

176 Elemental concentrations (total elemental counts) of Fe and K were measured in high resolution (every 2 cm) using an  
177 Avaatech<sup>TM</sup> X-Ray Fluorescence (XRF) Core Scanner at the Alfred-Wegener-Institute, Bremerhaven. Both Holes A and B of  
178 ODP Site 1239 were sampled. A nondestructive measuring technique was applied, allowing rapid semi-quantitative  
179 geochemical analysis of sediment cores (Richter et al., 2006). Several studies comparing XRF core scanner data to geochemical  
180 measurements on discrete samples showed that major elements such as Fe, Ca, and K can be precisely measured with the  
181 scanner in a non-destructive way (e.g. Tjallingii et al., 2007).

## 182 3 Results

183 Five groups were established with pollen taxa grouped according to their main ecological affinity (Table 1). The groups  
184 páramo, upper montane forest, lower montane forest, and lowland rainforest represent vegetation belts with different altitudinal  
185 ranges (Hooghiemstra, 1984). To track changes of humidity, an additional group named “Indicators of humid conditions” was  
186 established. This group includes those taxa which permanently need humid conditions to grow. Changes of the pollen

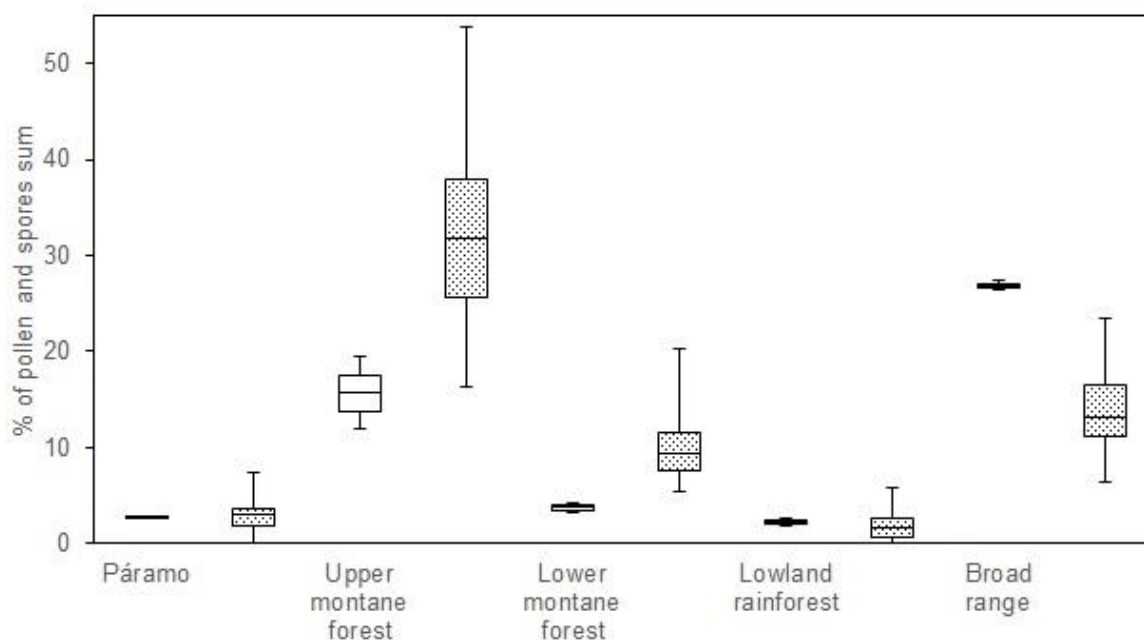




187 percentages of the ecological groups for the Pliocene interval and the core top samples are shown in Fig. 3. Pollen percentages  
188 of single taxa are shown in supplementary Fig. S1. Taxa that occurred in less than 10% of the samples were excluded from the  
189 interpretation.

### 190 3.1 Modern vs. Pliocene pollen assemblages

191 Fifty one different palynomorph types were recognized, including 29 pollen and 22 fern spore types. The samples are  
192 characterized by low pollen and spore concentrations of 685 and 465 grains/cm<sup>3</sup>, respectively. Indicators of humid conditions  
193 show intermediate values. Herbs and grass pollen are very abundant with 20–26%, but tree and shrub pollen decreased to 35–  
194 46% compared to the Pliocene interval. Broad range taxa reach their maximum abundance with 26–27%. Lowland rainforest  
195 and páramo pollen have similar representations as in the Pliocene, whereas the lower and upper montane forest pollen reach  
196 their lowest percentages. When compared to the Pliocene pollen composition, some floristic differences are seen, whereof the  
197 most prominent is the replacement of Podocarpaceae as the most abundant upper montane forest trees by *Alnus*. Another  
198 notable difference is the presence of *Rhizophora* pollen in one of the core top samples, whereas it is completely absent in the  
199 Pliocene interval.



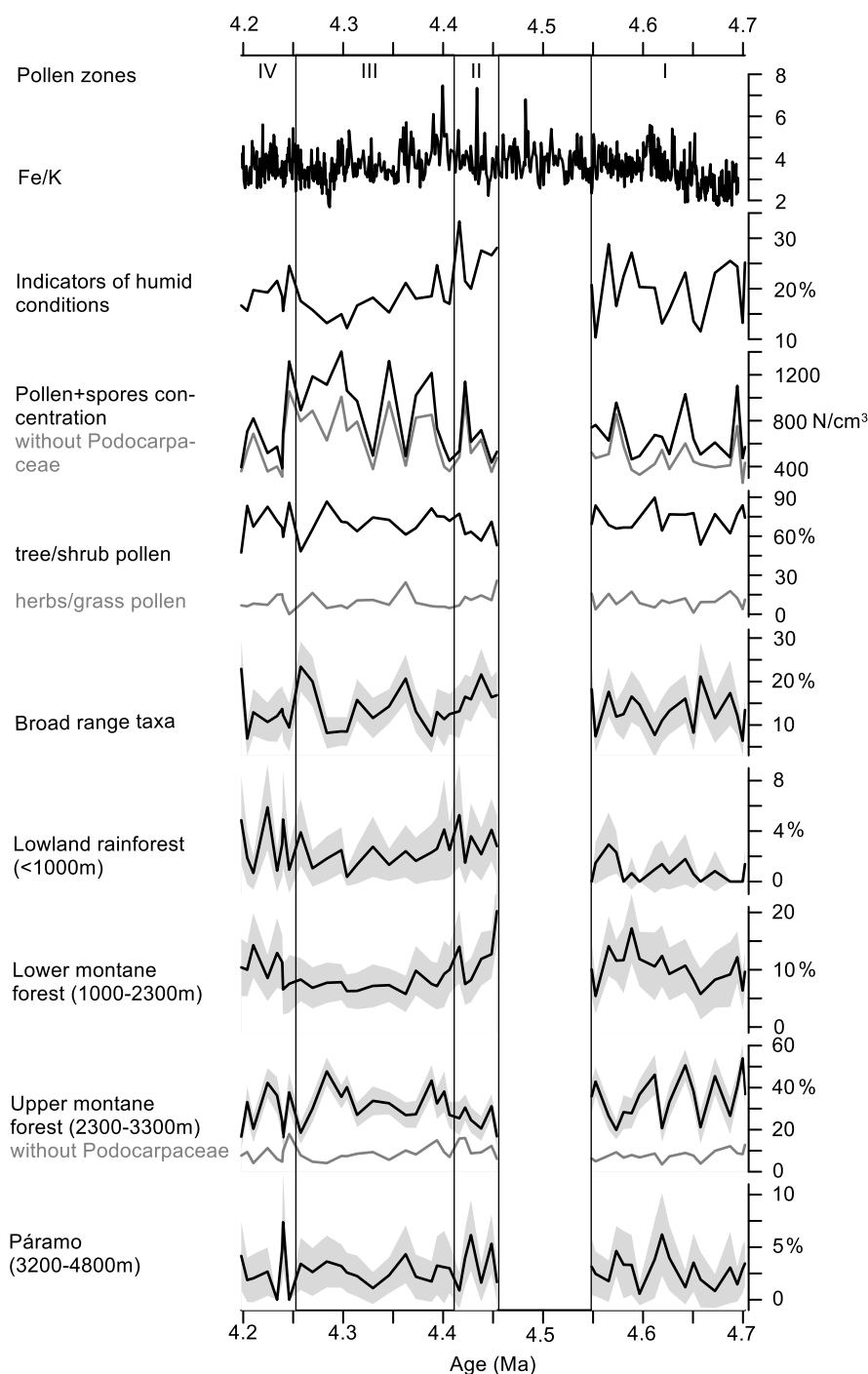
200

201 **Figure 3: Comparison of the relative percentages of the different vegetation belts between core top samples (left, plain) and Pliocene**  
202 **samples (right, dotted).**



### 203 **3.2 Description of the Pliocene pollen record**

204 In the Pliocene samples, 141 different palynomorph types were recognized, including 77 pollen and 64 fern spore types. A  
205 high percentage of tree and shrub pollen (46–88%) is present throughout the interval, compared to a low percentage of herbs  
206 and grass pollen (0–25%; Fig. 4). In most of the vegetation belts, one or two pollen or spore taxa are overrepresented. The  
207 lowland rainforest is mainly represented by Polypodiaceae, the lower montane forest is controlled by Cyatheaceae, and the  
208 upper montane forest is strongly influenced by Podocarpaceae and *Hedyosmum*. In the páramo, the percentages of the pollen  
209 taxa are evenly balanced. Of the total sum, the Andean forest pollen makes by far the largest percentage, with the upper  
210 montane forest ranging between 17 and 54% and the lower montane forest between 5 and 19%. The páramo is represented  
211 with 0 to 10% and the lowland rainforest with 0 to 6%. The remaining fraction has a wide or unknown ecological range.



212

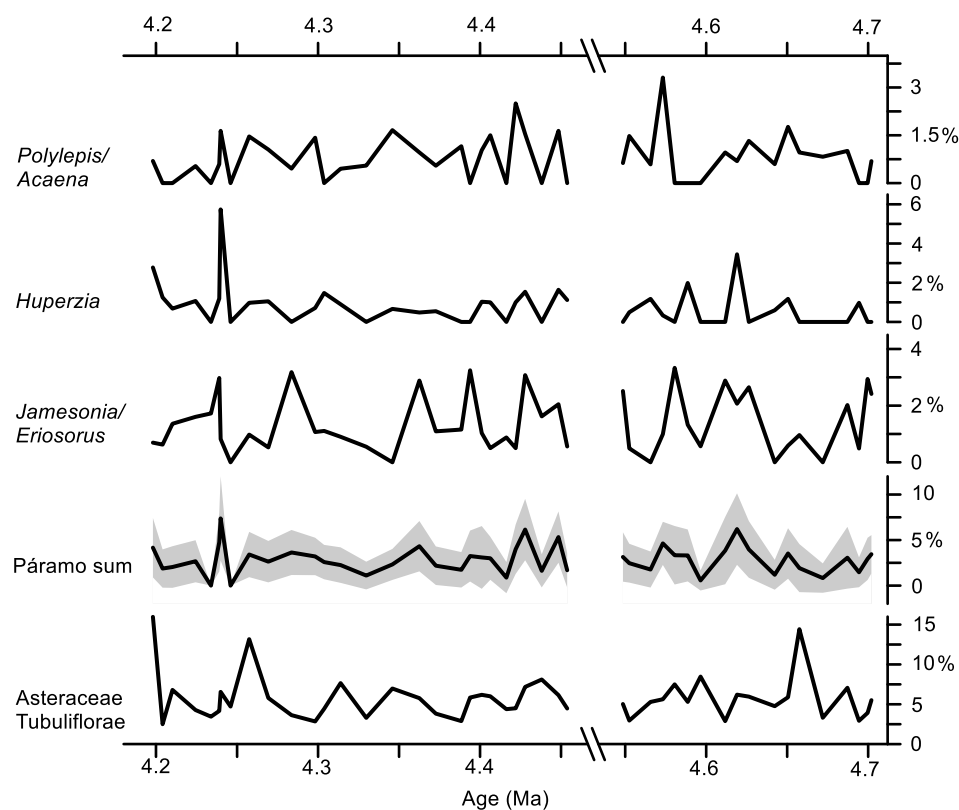
213 **Figure 4: Palynomorph percentages of ODP Hole 1239A for the four vegetation belts and other groups from 4.7 to 4.2 Ma. Grey**  
 214 **shading represents the 95% confidence intervals (after Maher, 1972). Vertical black lines delimit the pollen zones. On top elemental**  
 215 **ratios of Fe/K from Holes 1239A and 1239B. Ages are from Tiedemann et al. (2007). A hiatus is present in Hole 1239A between 4.45**  
 216 **and 4.55 Ma.**



217 The pollen record of ODP Hole 1239A was divided into four main pollen zones based on constrained cluster analysis. Pollen  
218 zone I (333.4–323.2 mbsf: 4.70–4.55 Ma, 18 samples) has low pollen and spores concentrations. It is characterized by increases  
219 in pollen values of lowland rainforest, lower montane forest, the percentage of fern spores, and the Fe/K ratio. The pollen  
220 concentrations of broad range taxa, upper montane forest, páramo, and indicators of humid conditions go through frequent  
221 fluctuations. Coastal desert herbs (Amaranthaceae) are well represented. Percentages of Poaceae pollen are low. Between  
222 pollen zone I and II, a hiatus of about 51.7 ka is present. In pollen zone II (319.4–316 mbsf: 4.45–4.42 Ma, 6 samples), the  
223 pollen and spores concentration is similar to pollen zone I. The lowland rainforest pollen, indicators of humid conditions, and  
224 the Fe/K ratio reach their maximum. Fern spores also reach their first maximum. Percentages of lower montane forest and  
225 páramo are high, whereas the percentage of upper montane forest is low at this time due to a strong decline of Podocarpaceae  
226 pollen. The representation of broad range taxa diminish in this interval, the decrease being mainly controlled by *Selaginella*,  
227 Cyperaceae, *Ambrosia/Xanthium*, and Amaranthaceae. Pollen zone III (316–305 mbsf: 4.41–4.26 Ma, 13 samples) shows a  
228 stepwise increase of the pollen and spores concentration with its maximum at 4.3 Ma. The concentration is strongly controlled  
229 by Podocarpaceae pollen which account for up to 44% of the pollen sum in this zone. The pollen of lowland rainforest, lower  
230 montane forest, páramo, indicators of humid conditions, and Fe/K show decreased percentages compared to zone II. Broad  
231 range taxa show some larger fluctuations. The upper montane forest pollen has its maximum extent of this zone (48%) at 4.28  
232 Ma due to the high percentage of Podocarpaceae. If the Podocarpaceae pollen are excluded from the upper montane forest, the  
233 representation of this vegetation belt shows the same pattern of decline as that of the lower montane forest and lowland  
234 rainforest. In pollen zone IV (305–301 mbsf: 4.25–4.2 Ma, 8 samples), the pollen and spores concentration decreases sharply  
235 after 4.24 Ma. The pollen percentage of lower montane forest increases. The percentage of fern spores is at its maximum in  
236 this zone. Percentages of páramo, upper montane forest, broad range taxa, indicators of humid conditions, and the Fe/K ratio  
237 remain similar as in zone III. The percentage of lowland rainforest pollen goes through frequent and large fluctuations.

### 238 3.3 Description of the páramo

239 The pollen spectrum from the páramo at ODP Site 1239 includes three different taxa which are mainly confined to the páramo:  
240 the pollen type *Polylepis/Acaena*, and the fern spores *Huperzia* and *Jamesonia/Eriosorus*. Other taxa which are characteristic  
241 of páramos, but cannot be exclusively attributed to this ecosystem because of their broad range occurrence were not included  
242 in the páramo sum (e.g. Asteraceae, Poaceae). The páramo sum constitutes up to 7% of the total pollen and spore sum, with  
243 the highest fractions found at 4.24 and 4.61 Ma, and lowest fractions around 4.23 and 4.59 Ma (Fig. 4). The pollen and spores  
244 types constituting the páramo show similar trends (Fig. 5), which supports the assumption of their common provenance.



245

246

247

248

**Figure 5: Development of the páramo. Páramo sum with 95% confidence intervals (grey shading). Asteraceae Tubuliflorae sum excluding *Ambrosia/Xanthium*-type for comparison. Ages are from Tiedemann et al. (2007). Break of axis represents a hiatus between 4.45 and 4.55 Ma.**

249

## 4 Discussion

250

### 4.1 The Holocene as modern reference

251

The core top samples indicate an expansion of broad range taxa and open vegetation, which happened on the expense of the montane forest being strongly diminished compared to the Pliocene situation. This together with the relatively low pollen concentrations would suggest drier conditions. Although there is no detailed age control on these surface/subsurface samples, a Holocene age can be assigned based on the benthic oxygen isotope record (Rincon-Martinez et al., 2010). A Holocene pollen record from nearby core TR 163-38 has high similarity to the core top samples in its youngest part, showing increased open vegetation (Poaceae, Cyperaceae, Asteraceae), low percentages of *Rhizophora*, maximum percentages of fern spores, and low pollen and spores concentrations (González et al., 2006). Despite the expansion of open vegetation, González et al. (2006) interpreted this record to reflect permanently humid conditions, with disturbance processes caused by human occupation and more intense fluvial dynamics. The relatively high percentage of indicators of humid conditions in the core top samples compared to pollen zones III and IV in the Pliocene would be in agreement with this interpretation. The core top samples from

259

260



261 ODP hole 1239B and the most recent part of core TR 163-38 are taken as a basis for the hydrological interpretation of the  
262 Pliocene pollen record.

## 263 **4.2 Climatic implications of vegetation change**

264 The presented marine palynological record provides new information on floristic and vegetation changes occurring along  
265 diverse ecological and climatic gradients through the early Pliocene. The consistently high percentage of tree and shrub pollen,  
266 compared to a low percentage of herbs and grass pollen (< 25%) suggests the predominance of forests and the nearly absence  
267 of open grasslands (below the forest line) during the early Pliocene. Moreover, the very low percentage of dry indicators  
268 (Amaranthaceae) suggests the absence of persisting drought conditions and supports the idea of a rather stable and humid  
269 climate that favored a closed forest cover. This is in good accordance with Pliocene climate models suggesting warmer and  
270 wetter conditions on most continents, which led to expansions of tropical forests and savannas at the expense of deserts  
271 (Salzmann et al., 2011). During the early Pliocene, no profound changes in the vegetation occur. All altitudinal vegetation  
272 belts are already present, with varying ratios. The representation of lowland rainforest goes through the most prominent  
273 development, from being almost absent to about 6% of the pollen sum.

274 Shifts in vegetation are caused by changes of various parameters such as temperature, precipitation, CO<sub>2</sub>, radiation, and they  
275 can rarely be explained by a single parameter but are a result of their complex interplay. It is therefore challenging to find the  
276 parameter which has the strongest influence on vegetation. All altitudinal vegetation belts (if Podocarpaceae are excluded)  
277 show a similar pattern of expansion and retreat over time, with an increase in pollen zone I, a maximum in pollen zone II,  
278 retreat in pollen zone III, and another maximum in pollen zone IV. It is known from other Andean pollen records (e.g.  
279 Hooghiemstra and Ran (1994)) that vegetation belts forced by temperature follow a pattern of opposing expansion and retreat.  
280 Such a pattern is seen here in the upper montane forest and the páramo belt (Fig. 5), but the more general pattern which  
281 comprises all vegetation belts seems to reflect changes in hydrology rather than temperature. In this respect, a synchronous  
282 increase/decrease in all vegetation belts is interpreted to reflect more humid/less humid conditions.

### 283 **4.2.1 Development of the coastal vegetation**

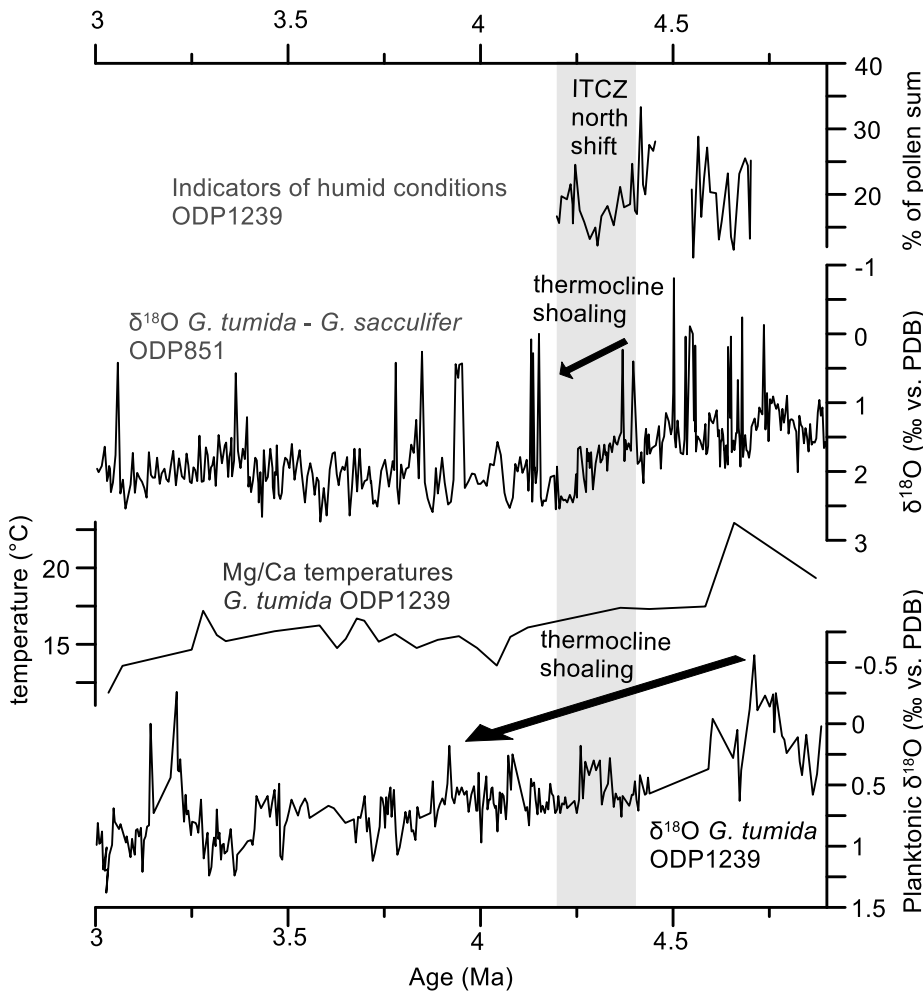
284 Pollen zones I and IV show an expansion of coastal desert herbs (Amaranthaceae, Fig. S1), which coincides with low SSTs at  
285 ODP Site 846 in the EEP, suggesting an influence of the Humboldt Current on the coastal vegetation of southern Ecuador.  
286 Remarkably, the lowland rainforest and the coastal desert herbs follow a similar trend. This seems odd at the first glance, but  
287 a possible mechanism to explain this pattern would invoke effects of El Niño. The main transport agent for pollen in this region  
288 are rivers, but in the coastal desert area of southern Ecuador and northern Peru, fluvial discharge rates are low (Milliman and  
289 Farnsworth, 2011). Therefore, pollen might be retained on land until an El Niño event causes severe flooding in the coastal  
290 areas (Rodbell et al., 1999) and episodically fills the rivers which transport the pollen to the ocean. The effects of El Niño seem  
291 to be strongest in pollen zones I and IV where pollen percentages of the lowland rainforest and coastal desert herbs, but also  
292 the upper montane forest, fluctuate most strongly. The lowland rainforest of the coastal plain further north is within the present-



293 day range of the ITCZ, and expanded from 4.7 Ma onwards possibly due to a southwards displacement of the mean latitude of  
294 the ITCZ (unpublished data from the earliest Pliocene show that the percentage of lowland rainforest before 4.7 Ma was very  
295 low). The development of the lowland rainforest also seems to be related to changes in eustatic sea level. High sea levels  
296 (Miller et al., 2005) coincide with peaks of the lowland rainforest in pollen zones II and IV.

#### 297 **4.2.2 Development of the montane vegetation**

298 Podocarpaceae strongly dominate the pollen spectrum in general, but the development of the pollen values is decoupled from  
299 that of all other taxa. This behavior can be explained if a different transport agent is considered. The high pollen production of  
300 Podocarpaceae and their specialized morphology (Regal, 1982) facilitate their eolian transport. In contrast, pollen from most  
301 other taxa is predominantly fluvially transported (González et al., 2006), therefore exhibiting a different pattern where high  
302 pollen concentrations correspond to high fluvial discharge in the source area. The eolian transport of Podocarpaceae explains  
303 the high pollen concentrations in pollen zone III, which occur despite less humid conditions compared to pollen zones II and  
304 IV. The increased eolian transport at 4.63 Ma and between 4.4 and 4.25 Ma is proposed here to be the result of an intensification  
305 of the easterly trade winds. Stronger easterlies also caused the shoaling of the thermocline in the EEP, as shown by models  
306 with a dynamic atmosphere (Zhang et al., 2012). The thermocline in the EEP shoaled between 4.8 and 4.0 Ma (Steph et al.,  
307 2006a, Fig. 6). Related to this process, a critical step of easterly trade wind intensification, indicated by increased eolian  
308 transport of Podocarpaceae pollen, occurred between 4.4 and 4.25 Ma.

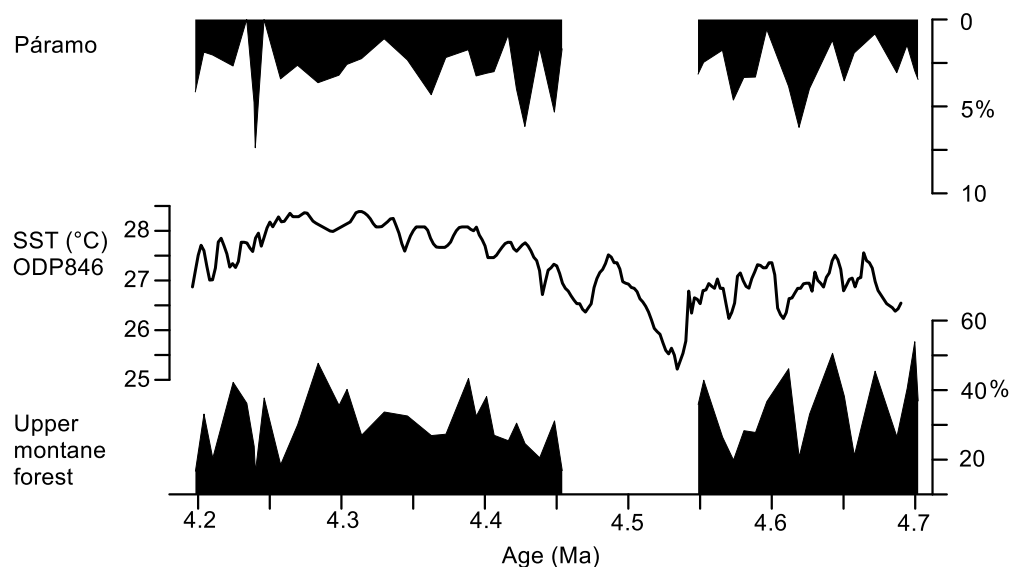


309

310 **Figure 6: Percentages of indicators of humid conditions (ODP Site 1239, this study), *G. tumida* – *G. sacculifer* difference in  $\delta^{18}\text{O}$  from**  
 311 **ODP Site 851 in the eastern equatorial Pacific (Cannariato and Ravelo, 1997), and *G. tumida* Mg/Ca temperatures and  $\delta^{18}\text{O}$  from**  
 312 **ODP Site 1239 (Steph, 2005; Steph et al., 2010). Grey shading marks the period of thermocline shoaling at ODP Site 851 and ITCZ**  
 313 **north shift.**

314 Another noteworthy oceanographic change occurred at 4.4 Ma in the EEP. Farrell et al. (1995) described a shift in the locus  
 315 of maximum opal accumulation rates from ODP Site 850 to ODP Site 846 (Galápagos region), caused by a shift in the  
 316 availability of nutrients, which is possibly related to increased trade wind strength after 4.4 Ma. Besides being influenced by  
 317 hydrological changes and wind strength, the upper montane forest and the páramo also respond to temperature changes.  
 318 Expansions of the upper montane forest combined with retreats of the páramo coincide with higher sea surface temperatures  
 319 in the EEP (ODP Site 846, Fig. 7). Warmer atmospheric temperatures cause an expansion of the upper montane forest to higher  
 320 altitudes, resulting in a reduction of the area occupied by páramo and therefore the decline of páramo pollen. On the other  
 321 hand, higher sea surface temperatures cause higher evaporation and thus higher orographic precipitation in the western Andean  
 322 Cordillera which might also play a role.





323

324

325

**Figure 7: Sums of upper montane forest and páramo, and UK'37 sea surface temperatures (SST) of ODP site 846 in the eastern equatorial Pacific (Lawrence et al., 2006).**

326

#### 4.3 Fe/K as a tracer for changes in fluvial runoff

327

328

329

330

331

332

333

334

335

336

337

338

339

340

The Fe/K ratio has been shown to be a suitable tracer to distinguish terrigenous input of slightly weathered material from drier regions from highly weathered material from humid tropical latitudes. Sediments from deeply chemically weathered terrains have higher iron concentrations compared to the more mobile potassium (Mulitza et al., 2008). Before paleoclimatic interpretations can be made based on elemental ratios, other processes which possibly influence the distribution of Fe/K in marine sediments should be examined, like changes of the topography of Andean river drainage basins, the input of mafic rock material, or diagenetic Fe remobilization (Govin et al., 2012). For northeastern South America it was shown that during the middle Miocene, uplift of the Eastern Andean Cordillera led to changes in the drainage direction of the Orinoco and Magdalena rivers and to the formation of the Amazon River (Hoorn, 1995). If a similar temporal history of uplift and changing drainage patterns is assumed for the western Andean Cordillera, the large-scale patterns of the present topography and river drainage basins should have been in place by the early Pliocene. Therefore, the main direction of fluvial transport of Fe should have been similar to today. Diagenetic alteration was shown not to affect Fe concentrations at Site 1239 (Rincon-Martinez, 2013). The Fe/K ratio therefore seems to be an adequate tracer of fluvial input at this study site. The trend of Fe/K is similar to the pattern of humidity inferred from the pollen spectrum, showing the highest values around 4.46 Ma, thus supporting the hydrological interpretation of the pollen record.

341

#### 4.4 Development of the páramo and implications for Andean uplift

342

343

In order to use páramo vegetation as an indicator for Andean elevation, the altitudinal restriction of the páramo taxa to environments above the forest line is a prerequisite. Although no true páramo endemics occurred in the marine samples, or



344 rather, they could not be identified due to the lack of genus-level morphological distinction (especially *Espeletia* from the  
345 Asteraceae and some Poaceae, e.g. *Festuca*), several taxa are mainly confined to high Andean environments. Dwarf trees of  
346 *Polylepis* typically form patches above the forest line and its natural altitudinal range is thought to occur between a lower limit  
347 which forms the transition to other forest types and up to 5000 m (Kessler, 2002). *Huperzia* occurs in montane forests as  
348 epiphytes and with terrestrial growth form in the páramo (Sklenar et al., 2011). *Jamesonia* and *Eriosorus* are both found in  
349 cool and wet highlands, with most species being found between 2200 and 5000 m (Sanchez and Baracaldo, 2004). Asteraceae  
350 are not restricted to the páramo, but their occurrence in the montane forest and in the lowland rainforest of the Pacific coast is  
351 scarce (Behling et al., 1998). With a contribution of up to 16% of the pollen sum, their source area can be attributed mainly to  
352 the páramo. Additionally, the fluctuations are similar to the other páramo taxa, which is another indication for their common  
353 source area.

354 The pollen record shows a continuous existence of páramo vegetation without changes in composition. During the warm  
355 Pliocene, the upper montane forest is assumed to have extended to similar or even higher altitudes as today. Despite this  
356 upward expansion of the upper montane forest, the páramo was still present, which implies that the western Cordillera of the  
357 northern Andes had already gone through substantial uplift by that time. Furthermore, the pollen record has a large montane  
358 signature, which would not be the case if the Andes had reached less than half of their modern height by the early Pliocene  
359 (Coltorti and Ollier, 2000). The upper montane forest which constitutes up to 60% of the pollen sum shows that montane  
360 habitats with the corresponding altitudinal belts were already existent. These findings suggest an earlier uplift history for the  
361 western Cordillera of the Northern Andes and according development of the high Andean páramo ecosystem than previously  
362 inferred from palynological studies of the eastern Cordillera in Colombia (Hooghiemstra et al., 2006; Van der Hammen et al.,  
363 1973). This might also be an indication that the uplift history of the western Cordillera of Ecuador is temporally more closely  
364 related to the uplift of the Central Andes where a major phase of uplift occurred between 10 and 6 Ma (Garzzone et al., 2008).  
365 In another recent palynological study, the arrival of palynomorphs from the páramo in sediments of the Amazon fan has been  
366 documented since 5.4 Ma (Hoorn et al., 2017). Since the Amazon has its westernmost source in Peru, this signal might be  
367 related to the uplift of the Central Andes. These new records also imply that the modern atmospheric circulation with the Andes  
368 acting as a climate divide has essentially been in place at least since the late Miocene/early Pliocene.

#### 369 **4.5 Comparing models and proxy data**

370 Several studies have suggested the existence of a “permanent El Niño” during the Pliocene (e.g. Fedorov et al., 2006; Wara et  
371 al., 2005). El Niño events are characterized by a shift in the Walker circulation, resulting in exceptionally heavy precipitation  
372 particularly over the lowlands of central and southern Ecuador (Bendix and Bendix, 2006) and simultaneous below-average  
373 rainfall over the northwestern slopes of the Andes (Vuille et al., 2000). A permanent El Niño-like climate state during the early  
374 Pliocene would thus have involved permanently humid conditions with high rates of precipitation and fluvial discharge in the  
375 lowlands. Such a climate would have favored the persistence of a broad rain forest coverage and precluded the development  
376 of the desert that exists in coastal southern Ecuador today. The presented pollen record indeed indicates very humid conditions



377 and the only indicator of dry vegetation is a small percentage of Amaranthaceae pollen. The predicted pattern of expansion of  
378 lowland rainforest at the cost of Andean forest during permanent El Niño is not reflected in the pollen record. Instead, all  
379 altitudinal vegetation belts go through simultaneous shifts of expansion and retreat.

380 The hypothesis of a permanent El Niño climate state involving a reduced zonal Pacific SST gradient has recently been  
381 questioned as SST reconstructions differ substantially depending on the method. Zhang et al. (2014) claim that a zonal  
382 temperature gradient of  $-3^{\circ}\text{C}$  has existed since the late Miocene and even intensified during the Pliocene. Our pollen record  
383 instead indicates an influence of periodic El Niño-related variations on the coastal and montane vegetation, especially between  
384 4.7 and 4.55 Ma and between 4.26 and 4.2 Ma, recorded by strong fluctuations in the pollen percentages of coastal and montane  
385 vegetation. The overall parallel expansion and retreat of all vegetation belts would make a more uniform shift in moisture  
386 supply a more likely explanation. Such a shift could be caused by a latitudinal displacement of the ITCZ. A southward  
387 displacement of the ITCZ over both Atlantic and Pacific has been proposed as a response to stronger zonal temperature and  
388 pressure gradients which developed after the restriction of the Central American Seaway and/or a weakening of Southern  
389 Hemisphere temperature gradients (Billups et al., 1999). The timing of the southward shift was narrowed down to 4.4 to 4.3  
390 Ma in this study, based on  $\delta^{18}\text{O}$  records of planktonic foraminifera. The pollen record suggests a slightly different timing, with  
391 a gradual southwards displacement of the ITCZ between 4.7 Ma and 4.42 Ma when the southernmost position was reached. A  
392 less humid phase, indicated by a decrease of humid indicators, lowland rainforest pollen, lower montane forest pollen, and the  
393 Fe/K ratio, followed between 4.42 and 4.26 Ma where the ITCZ presumably had a slightly more northern position. This phase  
394 coincides with the shoaling of the thermocline at ODP Site 851 in the eastern equatorial Pacific (Cannariato and Ravelo, 1997,  
395 Fig. 6). A southward displacement of the ITCZ during the early Pliocene would also be in accordance with eolian deposition  
396 patterns in the EEP which show a latitudinal shift in eolian grain-size and eolian flux between 6 and 4 Ma (Hovan, 1995). The  
397 rather small and slow changes in humidity imply that the ITCZ shift was a gradual process, rather than the response to a single  
398 threshold. Just like the Central American Seaway was restricted and reopened several times before its definitive closure at  
399 around 2.8 Ma (O’Dea et al., 2016), the atmospheric circulation might have adapted gradually in several small steps to these  
400 tectonic changes.

401 Numerical models suggesting a northward shift of the ITCZ in response to the closure of the Central American Seaway or the  
402 uplift of the northern Andes do not necessarily disagree with an early Pliocene southward shift inferred from proxy data. Both  
403 events occurred gradually over several millions of years and despite recent advances in constraining these events, the timing  
404 of major phases in the uplift histories are still debated. In the case of the Central American Seaway, the timing of surface water  
405 restriction based on diverging salinities in the Caribbean and Pacific ocean, respectively, is well constrained and numerous  
406 global oceanographic changes have been associated with it. Possibly these oceanic reorganizations did not directly trigger  
407 modifications of the atmospheric circulation, but critical periods of uplift influencing atmospheric circulation might have  
408 occurred earlier. On the other hand, the respective model sensitivity experiments generally only consider isolated changes in  
409 single boundary conditions (e.g. closed or open Central American Seaway). Therefore, the effect of those (i.e. a northward  
410 shift of the ITCZ) might counteract the general trend of a southward shift since the late Miocene due to a decrease in the



411 hemispheric temperature gradient (e.g. Pettke et al., 2002). Additionally, global coupled models exhibit uncertainties in the  
412 representation of ocean–atmosphere feedback and cloud–radiation feedbacks, which are especially strong in the study region  
413 (i.e. showing a double ITCZ and an extensive EEP cold tongue (Li and Xie, 2014)). This is problematic also in the light of the  
414 high sensitivity of the ITCZ position to slight shifts in the atmospheric energy balance (Schneider et al., 2014). Another aspect  
415 to consider is that whereas proxy records record the transient response of the climate system over a limited time period, the  
416 mentioned model simulations do not reproduce a stepwise process of environmental changes, e.g. following the closure of the  
417 Panama isthmus (i.e. the shoaling of the thermocline at ~ 4.8 – 4.0 Ma and the start of the EEP cold tongue at ~ 4.3 – 3.6 Ma,  
418 as according to Lawrence et al. (2006) and Steph et al. (2006a)), but the overall equilibrium response.

419 Concerning the uplift of the northern Andes, there is still a large uncertainty about the time when the Eastern Cordillera reached  
420 its current elevation. Paleobotanists (e.g. Hooghiemstra et al., 2006; Hoorn et al., 2010; Van der Hammen et al., 1973) and  
421 some tectonic geologists (e.g. Mora et al., 2008) argue for a rapid rise of the region since 4–6 Ma, while others conclude that  
422 this is rather unlikely implying an earlier uplift based on biomarker-based paleotemperatures (e.g. Anderson et al., 2015; Mora-  
423 Páez et al., 2016). The estimates for uplift of the Western Cordillera in Ecuador differ even more strongly, and range from  
424 rapid exhumation around 13 and 9 Ma based on thermochronology (Spikings et al., 2005) to a recent uplift during the Pliocene  
425 and Pleistocene (Coltorti and Ollier, 2000). Our pollen record from the páramo shows that the northern Andes must have  
426 already reached close to modern elevations by the early Pliocene. If an early Andean uplift is assumed, the atmospheric  
427 response predicted by the model would have occurred earlier, which would also be in agreement with proxy data indicating a  
428 northern position of the ITCZ during the late Miocene (Hovan, 1995).

429 Overall, even if the timing and identification of major steps in the shoaling and restriction of the Central American Seaway or  
430 in the uplift of the Northern Andes are resolved, the critical threshold for profound changes in atmospheric circulation and  
431 climate may have occurred at any time during the tectonic processes. Within the analyzed time window, large changes in  
432 atmospheric circulation which have been proposed as a response to the closure of the Central American Seaway (Ravelo et al.,  
433 2004) are absent.

## 434 5 Conclusions

- 435 1) Between 4.7 and 4.2 Ma, a permanently humid climate with broad rainforest coverage existed in western equatorial  
436 South America. No evidence was found for a permanent El Niño-like climate state, but strong fluctuations in the  
437 vegetation between 4.7 and 4.55 Ma and between 4.26 and 4.2 Ma indicate strong periodic El Niño variability at this  
438 time. Hydrological changes between 4.55 and 4.26 Ma are attributed to gradual shifts of the Intertropical Convergence  
439 Zone which reached its southernmost position around 4.42 Ma and shifted slightly north afterwards.
- 440 2) The most prominent shift in the vegetation occurred in the lowland rainforest.
- 441 3) Between 4.41 and 4.26 Ma, an increased eolian influx of Podocarpaceae pollen indicates an increased strength of the  
442 easterly trade winds, which is presumably related to the shoaling of the EEP thermocline.



- 443 4) Results from proxy data and numerical modelling studies regarding the position of the ITCZ during the early Pliocene  
444 are not necessarily contradictory. Considering the temporal uncertainties regarding major steps of CAS closure and  
445 uplift of the northern Andes, the proposed northward shift of the ITCZ in response to these events might have occurred  
446 much earlier (e.g. during the middle to late Miocene).
- 447 5) The continuous presence of páramo vegetation implies that by the early Pliocene, the western Cordillera of the  
448 northern Andes had already reached an elevation suitable for the development of vegetation above the upper forest  
449 line. This new paleobotanical evidence points towards an earlier uplift of the northern Andes than previously  
450 suggested by terrestrial paleobotanical records.

451

#### 452 Data availability

453 The underlying research data can be accessed via <https://pangaea.de/>.

454

#### 455 Author contribution

456 L. Dupont and F. Grimmer conceived the idea, and L. Dupont, F. Grimmer and F. Lamy carried out the analyses. F. Grimmer  
457 prepared the manuscript with contributions from all co-authors.

458

#### 459 Competing interests

460 The authors declare that they have no conflict of interest.

461

#### 462 Acknowledgements

463 This project was funded by the Deutsche Forschungsgemeinschaft (DFG) through the TROPSAP project (DU221/6) and via  
464 the DFG Research Center / Cluster of Excellence “The Ocean in the Earth System — MARUM”. The first author thanks  
465 GLOMAR – Bremen International Graduate School for Marine Sciences, University of Bremen, Germany, for support. The  
466 IODP Gulf Coast Repository (GCR) we acknowledge for their assistance in providing the core samples.

467

#### 468 References

- 469 Anderson, V. J., Saylor, J. E., Shanahan, T. M., and Horton, B. K.: Paleoelevation records from lipid biomarkers:  
470 Application to the tropical Andes, *Geological Society of America Bulletin*, 127, 1604-1616, 2015.
- 471 Balslev, H.: Distribution Patterns of Ecuadorean Plant-Species, *Taxon*, 37, 567-577, 1988.
- 472 Bartoli, G., Sarnthein, M., Weinelt, M., Erlenkeuser, H., Garbe-Schönberg, D., and Lea, D. W.: Final closure of  
473 Panama and the onset of northern hemisphere glaciation, *Earth and Planetary Science Letters*, 237, 33-44, 2005.
- 474 Behling, H., Hooghiemstra, H., and Negret, A. J.: Holocene history of the Choco Rain Forest from Laguna Piusbi,  
475 Southern Pacific Lowlands of Colombia, 1998. 1998.
- 476 Bendix, A. and Bendix, J.: Heavy rainfall episodes in Ecuador during El Nino events and associated regional  
477 atmospheric circulation and SST patterns, *Advances in Geosciences*, 6, 43-49, 2006.



- 478 Bendix, J. and Lauer, W.: Die Niederschlagsjahreszeiten in Ecuador und ihre Klimadynamische Interpretation,  
479 1992. 1992.
- 480 Billups, K., Ravelo, A. C., Zachos, J. C., and Norris, R. D.: Link between oceanic heat transport thermohaline  
481 circulation and the Intertropical Convergence Zone in the early Pliocene Atlantic, *Geology*, 24, 319-322, 1999.
- 482 Bush, M. B. and Weng, C.: Introducing a new (freeware) tool for palynology, *Journal of Biogeography*, 34, 377-  
483 380, 2007.
- 484 Cannariato, K. G. and Ravelo, A. C.: Pliocene-Pleistocene evolution of eastern tropical Pacific surface water  
485 circulation and thermocline depth, *Paleoceanography*, 12, 805-820, 1997.
- 486 Colinvaux, P., De Oliveira, P. E., and Moreno Patino, J. E.: Amazon Pollen Manual and Atlas, 1999.
- 487 Coltorti, M. and Ollier, C. D.: Geomorphic and tectonic Evolution of the Ecuadorian Andes, *Geomorphology*, 32,  
488 1-19, 2000.
- 489 Corredor, F.: Eastward extent of the Late Eocene-Early Oligocene onset of deformation across the northern Andes:  
490 constraints from the northern portion of the Eastern Cordillera fold belt, Colombia, *Journal of South American  
491 Earth Sciences*, 16, 445-457, 2003.
- 492 Farrell, J. W., Raffi, I., Janecek, T. R., Murray, D. W., Levitan, M., Dadey, K. A., Emeis, K.-C., Lyle, M., Flores, J. A.,  
493 and Hovan, S.: Late Neogene Sedimentation Patterns in the eastern equatorial Pacific Ocean, *Proceedings of the  
494 Ocean Drilling Program, Scientific Results*, 138, 1995.
- 495 Fedorov, A. V., Dekens, P. S., McCarthy, M., Ravelo, A. C., deMenocal, P. B., Barreiro, M., Pacanowski, R. C., and  
496 Philander, S. G.: The Pliocene paradox (mechanisms for a permanent El Niño), *Science*, 312, 1485-1489, 2006.
- 497 Feng and Poulsen, C. J.: Andean elevation control on tropical Pacific climate and ENSO, *Paleoceanography*, 29,  
498 795-809, 2014.
- 499 Flantua, S., Hooghiemstra, H., Van Boxel, J. H., Cabrera, M., González-Carranza, Z., and González-Arango, C.:  
500 Connectivity dynamics since the last glacial maximum in the northern Andes a pollen driven framework to assess  
501 potential migration, 2014. 2014.
- 502 Flohn, H.: A hemispheric circulation asymmetry during Late Tertiary, *Geologische Rundschau*, 70, 725-736, 1981.
- 503 Garzzone, C. N., Hoke, G. D., Libarkin, J. C., Withers, S., MacFadden, B., Eiler, J., Ghosh, P., and Mulch, A.: Rise of  
504 the Andes, *Science*, 320, 1304-1307, 2008.
- 505 Gentry, A. H.: Species richness and floristic composition of Chocó region plant communities, *Caldasia*, 15, 71-91,  
506 1986.
- 507 González, C., Urrego, L. E., and Martínez, J. I.: Late Quaternary vegetation and climate change in the Panama  
508 Basin: Palynological evidence from marine cores ODP 677B and TR 163-38, *Palaeogeography, Palaeoclimatology,  
509 Palaeoecology*, 234, 62-80, 2006.
- 510 Govin, A., Holzwarth, U., Heslop, D., Ford Keeling, L., Zabel, M., Mulitza, S., Collins, J. A., and Chiessi, C. M.:  
511 Distribution of major elements in Atlantic surface sediments (36°N-49°S): Imprint of terrigenous input and  
512 continental weathering, *Geochemistry, Geophysics, Geosystems*, 13, n/a-n/a, 2012.
- 513 Gregory-Wodzicki, K. M.: Uplift history of the Central and Northern Andes: A review, *Geological Society of America  
514 Bulletin*, 112, 1091-1105, 2000.
- 515 Grimm, E.: *Tilia and Tiliagraph*, Illinois State Museum, Springfield, 1991. 1991.
- 516 Groeneveld, J., Hathorne, E. C., Steinke, S., DeBey, H., Mackensen, A., and Tiedemann, R.: Glacial induced closure  
517 of the Panamanian Gateway during Marine Isotope Stages (MIS) 95-100, *Earth and Planetary Science Letters*,  
518 404, 296-306, 2014.
- 519 Haug, G. H. and Tiedemann, R.: Effect of the formation of the Isthmus of Panama on Atlantic Ocean thermohaline  
520 circulation, *Nature*, 393, 673-676, 1998.



- 521 Haug, G. H., Tiedemann, R., Zahn, R., and Ravelo, A. C.: Role of Panama uplift on oceanic freshwater balance,  
522 *Geology*, 29, 207-210, 2001.
- 523 Hooghiemstra, H.: Vegetational and Climatic History of the High Plain of Bogotá, Colombia: A Continuous Record  
524 of the Last 3.5 Million Years, A.R. Gantner Verlag K.G., Vaduz, 1984.
- 525 Hooghiemstra, H. and Ran, E. T. H.: Upper and middle Pleistocene climatic change and forest development in  
526 Colombia pollen record Funza II, *Palaeogeography, Palaeoclimatology, Palaeoecology*, 109, 211-246, 1994.
- 527 Hooghiemstra, H., Wijninga, V. M., and Cleef, A. M.: The Paleobotanical Record of Colombia: Implications for  
528 Biogeography and Biodiversity<sup>1</sup>, *Annals of the Missouri Botanical Garden*, 93, 297-325, 2006.
- 529 Hoorn, C.: Andean tectonics as a cause for changing drainage patterns in Miocene northern South America, 1995.  
530 1995.
- 531 Hoorn, C., Bogotá-A., G. R., Romero-Baez, M., Lammertsma, E. I., Flantua, S., Dantas, E. L., Dino, R., do Carmo, D.  
532 A., and Chemale Jr, F.: The Amazon at sea: Onset and stages of the Amazon River from a marine record, with  
533 special reference to Neogene plant turnover in the drainage basin, *Global and Planetary Change*, 2017. 2017.
- 534 Hoorn, C. and Flantua, S.: Geology. An early start for the Panama land bridge, *Science*, 348, 186-187, 2015.
- 535 Hoorn, C., Wesselingh, F. P., ter Steege, H., Bermudez, M. A., Mora, A., Sevink, J., Sanmartin, I., Sanchez-Meseguer,  
536 A., Anderson, C. L., Figueiredo, J. P., Jaramillo, C., Riff, D., Negri, F. R., Hooghiemstra, H., Lundberg, J., Stadler, T.,  
537 Sarkinen, T., and Antonelli, A.: Amazonia through time: Andean uplift, climate change, landscape evolution, and  
538 biodiversity, *Science*, 330, 927-931, 2010.
- 539 Hovan: Late Cenozoic Atmospheric Circulation Intensity and climatic history recorded by eolian deposition in the  
540 eastern equatorial pacific ocean Leg138, 1995. 1995.
- 541 Jørgensen, P. M., León-Yáñez, S., and Missouri Botanical Garden.: Catalogue of the vascular plants of Ecuador =  
542 Catálogo de las plantas vasculares del Ecuador, Missouri Botanical Garden Press, St. Louis, Mo., 1999.
- 543 Kessler, M.: The "Polylepis problem": Where do we stand?, *Ecotropica*, 8, 97-110, 2002.
- 544 Lawrence, K. T., Liu, Z., and Herbert, T. D.: Evolution of the eastern tropical Pacific through Plio-Pleistocene  
545 glaciation, *Science*, 312, 79-83, 2006.
- 546 Li, G. and Xie, S. P.: Tropical Biases in CMIP5 Multimodel Ensemble: The Excessive Equatorial Pacific Cold Tongue  
547 and Double ITCZ Problems, *Journal of Climate*, 27, 1765-1780, 2014.
- 548 Lunt, D. J., Valdes, P. J., Haywood, A., and Rutt, I. C.: Closure of the Panama Seaway during the Pliocene:  
549 implications for climate and Northern Hemisphere glaciation, *Climate Dynamics*, 30, 1-18, 2008.
- 550 Luteyn, J. L.: Páramos, *Memoirs of The New York Botanical Garden*, 1999.
- 551 Maher, L. J.: Nomograms for computing 0.95 confidence limits of pollen data, *Review of Palaeobotany and*  
552 *Palynology*, 13, 85-93, 1972.
- 553 Marchant, R., Almeida, L., Behling, H., Berrio, J. C., Bush, M., Cleef, A., Duivenvoorden, J., Kappelle, M., De Oliveira,  
554 P., Teixeira de Oliveira-Filho, A., Lozano-Garcia, S., Hooghiemstra, H., Ledru, M.-P., Ludlow-Wiechers, B.,  
555 Markgraf, V., Mancini, V., Paez, M., Prieto, A., Rangel, O., and Salgado-Labouriau, M.: Distribution and ecology of  
556 parent taxa of pollen lodged within the Latin American Pollen Database, *Review of Palaeobotany and Palynology*,  
557 121, 1-75, 2002.
- 558 Miller, K. G., Kominz, M. A., Browning, J. V., Wright, J. D., Mountain, G. S., Katz, M. E., Sugarman, P. J., Cramer, B.  
559 S., Christie-Blick, N., and Pekar, S. F.: The Phanerozoic record of global sea-level change, *Science*, 310, 1293-1298,  
560 2005.
- 561 Milliman, J. D. and Farnsworth, K. L.: River discharge to the coastal ocean : a global synthesis, Cambridge  
562 University Press, Cambridge ; New York, 2011.
- 563 Mix, A., Tiedemann, R., and Blum, P.: Proceedings of the Ocean Drilling Program, Initial Reports, 202, 2003.



- 564 Montes, C.: Middle Miocene closure of the Central American Seaway, 2015. 2015.
- 565 Mora-Páez, H., Mencin, D. J., Molnar, P., Diederix, H., Cardona-Piedrahita, L., Peláez-Gaviria, J.-R., and Corchuelo-  
566 Cuervo, Y.: GPS velocities and the construction of the Eastern Cordillera of the Colombian Andes Geophysical  
567 Research Letters Volume 43, Issue 16. In: Geophysical Research Letters, 16, 2016.
- 568 Mora, A., Parra, M., Strecker, M. R., Sobel, E. R., Hooghiemstra, H., Torres, V., and Jaramillo, J. V.: Climatic forcing  
569 of asymmetric orogenic evolution in the Eastern Cordillera of Colombia, GSA Bulletin, 120, 930-949, 2008.
- 570 Mülitz, S., Prange, M., Stuut, J. B., Zabel, M., von Döbenek, T., Itambi, A. C., Nizou, J., Schulz, M., and Wefer, G.:  
571 Sahel megadroughts triggered by glacial slowdowns of Atlantic meridional overturning, Paleoclimatology, 23,  
572 2008.
- 573 Murillo, M. T. and Bless, M. J. M.: Spores of recent Colombian Pteridophyta I Trilete Spores, Review of  
574 Palaeobotany and Palynology, 1974. 1974.
- 575 Murillo, M. T. and Bless, M. J. M.: Spores of recent Colombian Pteridophyta II Monolet Spores, Review of  
576 Palaeobotany and Palynology, 1978. 1978.
- 577 O’Dea, A., Lessios, A. H., Coates, A. G., Eytan, R. I., Restrepo-Moreno, S. A., Cione, A. L., Collins, L. S., de Queiroz,  
578 A., Farris, D. W., Norris, R. D., Stallard, R. F., Woodburne, M. O., Aguilera, O., Aubry, M.-P., Berggren, W. A., Budd,  
579 A. F., Cozzuol, M. A., Coppard, S. E., Duque-Caro, H., Finnegan, S., Gasparini, G. M., Grossman, E. L., Johnson, K.  
580 G., Keigwin, L. D., Knowlton, N., Leigh, E. G., Leonard-Pingel, J. S., Marko, P. B., Pyenson, N. D., Ravello-Dolmen,  
581 P. G., Soibelzon, E., Soibelzon, L., Todd, J. A., Vermeij, G. J., and Jackson, J. B. C.: Formation of the Isthmus of  
582 Panama, Science Advances, 2, 2016.
- 583 Pettke, T., Halliday, A. N., and Rea, D. K.: Cenozoic evolution of Asian climate and sources of Pacific seawater Pb  
584 and Nd derived from eolian dust of sediment core LL44-GPC3, Paleoclimatology, 17, 2002.
- 585 Pisias, N.: Paleoclimatology of the eastern equatorial Pacific during the Neogene: Synthesis of Leg 138 drilling  
586 results, Proceedings of the Ocean Drilling Program, Scientific Results, 138, 5-21, 1995.
- 587 Ravello, A. C., Andreasen, D. H., Lyle, M. W., Lyle, A. O., and Wara, M. W.: Regional climate shifts caused by gradual  
588 global cooling in the Pliocene epoch, 2004. 2004.
- 589 Regal, P. J.: Pollination by Wind and Animals: Ecology of Geographic Patterns, Annual Review of Ecology and  
590 Systematics, 13, 497-524, 1982.
- 591 Richter, T. O., van der Gaast, S., Koster, B., Vaars, A., Gieles, R., de Stigter, H. C., de Haas, H., and van Weering, T.  
592 C. E.: The Avaatech XRF Core Scanner: Technical description and applications to NE Atlantic sediments. In: New  
593 Techniques in Sediment Core Analysis, Rothwell, R. G. (Ed.), Geol. Soc. Spec. Publ., 2006.
- 594 Rincon-Martinez, D.: Thesis, 2013. 2013.
- 595 Rincon-Martinez, D., Lamy, F., Contreras, S., Leduc, G., Bard, E., Saukel, C., Blanz, T., Mackensen, A., and  
596 Tiedemann, R.: More humid interglacials in Ecuador during the past 500 kyr linked to latitudinal shifts of the  
597 equatorial front and the Intertropical Convergence Zone in the eastern tropical Pacific, Paleoclimatology, 25,  
598 2010.
- 599 Rodbell, D. T., Seltzer, G. O., Anderson, D. M., Abbott, M. B., Enfield, D. B., and Newman, J. H.: An similar to 15,000-  
600 year record of El Niño-driven alluviation in southwestern Ecuador, Science, 283, 516-520, 1999.
- 601 Roubik, D. W. and Moreno, P.: Pollen and spores of Barro Colorado Island [Panama], Monographs in systematic  
602 botany from the Missouri Botanical Garden, 36, 1991.
- 603 Salzmann, U., Williams, M., Haywood, A. M., Johnson, A. L. A., Kender, S., and Zalasiewicz, J.: Climate and  
604 environment of a Pliocene warm world, Palaeogeography, Palaeoclimatology, Palaeoecology, 309, 1-8, 2011.
- 605 Sanchez and Baracaldo: Phylogenetics and biogeography of the neotropical fern genera Jamesonia and Eriosorus  
606 (Pteridaceae), 2004. 2004.





- 607 Schneider, T., Bischoff, T., and Haug, G. H.: Migrations and dynamics of the intertropical convergence zone,  
608 Nature, 513, 45-53, 2014.
- 609 Seilles, B., Goni, M. F. S., Ledru, M. P., Urrego, D. H., Martinez, P., Hanquiez, V., and Schneider, R.: Holocene land-  
610 sea climatic links on the equatorial Pacific coast (Bay of Guayaquil, Ecuador), Holocene, 26, 567-577, 2016.
- 611 Sklenar, P., Duskova, E., and Balslev, H.: Tropical and Temperate: Evolutionary History of Paramo Flora, Bot Rev,  
612 77, 71-108, 2011.
- 613 Sklenar, P. and Jorgensen, P. M.: Distribution patterns of Paramo Plants in Ecuador, Journal of Biogeography, 26,  
614 681-691, 1999.
- 615 Spikings, R. A., Winkler, W., Hughes, R. A., and Handler, R.: Thermochronology of allochthonous terranes in  
616 Ecuador: Unravelling the accretionary and post-accretionary history of the Northern Andes, Tectonophysics, 399,  
617 195-220, 2005.
- 618 Steph, S.: Pliocene Stratigraphy and the impact of Panama Uplift on changes in caribbean and tropical east pacific  
619 upper ocean stratification, 2005. 2005.
- 620 Steph, S., Tiedemann, R., Groeneveld, J., Sturm, A., and Nürnberg, D.: Pliocene Changes in Tropical East Pacific  
621 Upper Ocean Stratification: Response to Tropical Gateways?, Proceedings of the Ocean Drilling Program, Scientific  
622 Results, 202, 2006a.
- 623 Steph, S., Tiedemann, R., Prange, M., Groeneveld, J., Nurnberg, D., Reuning, L., Schulz, M., and Haug, G. H.:  
624 Changes in Caribbean surface hydrography during the Pliocene shoaling of the Central American Seaway,  
625 Paleoceanography, 21, 2006b.
- 626 Steph, S., Tiedemann, R., Prange, M., Groeneveld, J., Schulz, M., Timmermann, A., Nürnberg, D., Rühlemann, C.,  
627 Saukel, C., and Haug, G. H.: Early Pliocene increase in thermohaline overturning: A precondition for the  
628 development of the modern equatorial Pacific cold tongue, Paleoceanography, 25, n/a-n/a, 2010.
- 629 Takahashi, K. and Battisti, D. S.: Processes Controlling the Mean Tropical Pacific Precipitation Pattern. Part I: The  
630 Andes and the Eastern Pacific ITCZ, Journal of Climate, 20, 3434-3451, 2007.
- 631 Tiedemann, R., Sturm, A., Steph, S., Lund, S. P., and Stoner, J. S.: Astronomically calibrated timescales from 6 to  
632 2.5 Ma and benthic isotope stratigraphies, sites 1236, 1237, 1239, and 1241, Proceedings of the Ocean Drilling  
633 Program, Scientific Results, 202, 2007.
- 634 Tjallingii, R., Röhl, U., Kölling, M., and Bickert, T.: Influence of the water content on X-ray fluorescence core-  
635 scanning measurements in soft marine sediments, Geochemistry, Geophysics, Geosystems, 8, 2007.
- 636 Twilley, R. R., Cárdenas, W., Rivera-Monroy, V. H., Espinoza, J., Suescum, R., Armijos, M. M., and Solórzano, L.:  
637 The Gulf of Guayaquil and the Guayas River Estuary, Ecuador. In: Coastal Marine Ecosystems of Latin America,  
638 Seeliger, U. and Kjerfve, B. (Eds.), Springer, Heidelberg, 2001.
- 639 Van der Hammen, T., Werner, J. H., and van Dommelen, H.: Palynological record of the upheaval of the Northern  
640 Andes: a study of the Pliocene and Lower Quaternary of the Colombian early evolution of its high-Andean biota,  
641 Review of Palaeobotany and Palynology, 16, 1-122, 1973.
- 642 Vuille, M., Bradley, R. S., and Keimig, F.: Climate variability in the Andes of Ecuador and its relation to tropical  
643 Pacific and Atlantic Sea surface temperature anomalies, Journal of Climate, 2000. 2000.
- 644 Wara, M. W., Ravelo, A. C., and Delaney, M. L.: Permanent El Nino-like conditions during the Pliocene warm  
645 period, Science, 309, 758-761, 2005.
- 646 Zhang, X., Prange, M., Steph, S., Butzin, M., Krebs, U., Lunt, D. J., Nisancioglu, K. H., Park, W., Schmittner, A.,  
647 Schneider, B., and Schulz, M.: Changes in equatorial Pacific thermocline depth in response to Panamanian seaway  
648 closure: Insights from a multi-model study, Earth and Planetary Science Letters, 2012. 76-84, 2012.



649 Zhang, Y. G., Pagani, M., and Liu, Z.: A 12-million-year temperature history of the tropical Pacific Ocean, *Science*,  
650 344, 84-87, 2014.

651

652

653

654

655

656

657

658

659

660

661

662

663

664

665

666

667

668

669

670

671

672

673

674

675

676

677

678

679

680

681

682



683  
684  
685

**Table 1: List of identified pollen and spore taxa in marine ODP Holes 1239A (Pliocene samples) and 1239B (core top samples, taxa in grey occurred only in core top samples) and grouping according to their main ecological affinity (Flantua et al., 2014; Marchant et al., 2002).**

<b>Páramo</b>	<b>Upper montane forest</b>	<b>Lower montane forest</b>	<b>Lowland rainforest</b>	<b>Broad range taxa</b>	<b>Humid indicators</b>
<i>Polylepis/Acaena</i>	Podocarpaceae	Urticaceae/ Moraceae	Areaceae	Poaceae	Cyperaceae
<i>Jamesonia/Eriosorus</i>	<i>Hedyosmum</i>	<i>Erythrina</i>	Polypodiaceae	Cyperaceae	<i>Ranunculus</i>
<i>Huperzia</i>	<i>Clethra</i>	<i>Alchornea</i>	<i>Pityrogramma-Pteris altissima T</i>	Tubuliflorae (Asteraceae)	<i>Hedyosmum</i>
<i>Ranunculus</i>	<i>Myrica</i>	<i>Styloceras T</i>	<i>Wallichia</i>	Amaranthaceae	<i>Ilex</i>
<i>Draba</i>	Acanthaceae	Malpighiaceae		Rosaceae	<i>Pachira</i>
<i>Sisyrinchium</i>	Melastomataceae	Cyatheaceae		<i>Ambrosia/Xanthium</i>	<i>Myrica</i>
<i>Cystopteris diaphana T</i>	<i>Daphnopsis</i>	<i>Vernonia T</i>		Ericaceae	Malpighiaceae
	<i>Bocconia</i>	<i>Pteris grandifolia T</i>		<i>Artemisia</i>	Cyatheaceae
	<i>Myrsine</i>	<i>Pteris podophylla T</i>		<i>Ilex</i>	<i>Selaginella</i>
	<i>Lophosoria</i>	<i>Saccoloma elegans T</i>		<i>Thevetia</i>	<i>Pityrogramma-Pteris altissima T</i>
	<i>Elaphoglossum</i>	<i>Thelypteris</i>		<i>Salacia</i>	<i>Hymenophyllum T</i>
	<i>Hypolepis hostilis T</i>	<i>Ctenitis subincisa T</i>		Bromeliaceae	<i>Thelypteris</i>
	<i>Grammitis</i>			Malvaceae	<i>Ctenitis subincisa T</i>
	<i>Dodonaea viscosa</i>			Euphorbiaceae	<i>Alnus</i>



*Alnus*

*Liliaceae*

*Cystopteris*

*diaphana T*

Lycopodiaceae

excl. *Huperzia*

*Selaginella*

*Hymenophyllum*

*T*

*Calandrinia*